Structural Basis for the Glucocorticoid Response in a Mutant Human Androgen Receptor (AR^{ccr}) Derived from an Androgen-Independent Prostate Cancer

Pedro M. Matias,[†] Maria Arménia Carrondo,*[,†] Ricardo Coelho,[†] Monica Thomaz,[‡] Xiao-Yan Zhao,[#] Anja Wegg,[§] Kerstin Crusius,[§] Ursula Egner,[§] and Peter Donner[§]

Instituto de Tecnologia Química e Biológica, Universidade Nova de Lisboa, Apartado 127, 2780 Oeiras, Portugal, Instituto de Biologia Experimental e Tecnológica, Apartado 12, 2780 Oeiras, Portugal, Berlex Biosciences, P.O. Box 4099, Richmond, California 94804, and Schering AG Research Laboratories, 13342 Berlin, Germany

Received October 24, 2001

The crystal structure of a mutant androgen receptor (AR) ligand-binding domain (LBD) in complex with the agonist 9α-fluorocortisol has been determined at 1.95 Å resolution. This mutant AR contains two mutations (L701H and T877A) and was previously reported as a high-affinity cortisol/cortisone responsive AR (AR^{ccr}) isolated from the androgen-independent human prostate cancer cell lines MDA PCa 2a and 2b (Zhao et al. *Nature Med.* **2000**, *6*, 703−6). The three-dimensional structure of the AR^{ccr} LBD complexed with 9α-fluorocortisol shows the typical conformation of an agonist-bound nuclear receptor in which helix 12 is precisely positioned as a "lid" for the ligand-binding pocket. Binding of 9α-fluorocortisol to the AR^{ccr} involves favorable hydrogen bond patterns on the C17 and C21 substituents of the ligand due to the mutations at 701 and 877 in the AR^{ccr}. Our studies provide the first structural explanation for the glucocorticoid activation of AR^{ccr}, which is important for the development of new therapeutic treatments for androgen-independent prostate cancer.

Introduction

The progression of human prostate cancer is often linked with a high level of androgen receptor (AR) expression or mutations.[1−3] Androgen ablation therapy is the most effective treatment for patients suffering from metastatic prostate cancer since the growth of the tumor is initially androgen-dependent. But in the course of progression, prostate cancer cells switch from an androgen-dependent into an androgen-independent state. This transition is not well-understood.

Recently, a mutated AR has been isolated and characterized[4−6] from the androgen-independent prostate tumor cell lines MDA PCa 2a and 2b which were established from a bone metastasis of a patient whose prostate cancer exhibited androgen-independent growth.[7] The mutated AR contains two mutations (L701H and T877A) located in the ligand-binding domain (LBD) of the AR in the vicinity of the D-ring area of a steroidal ligand. This double mutant AR is highly sensitive toward cortisol and cortisone in binding and transactivation assays and is designated as the cortisol/cortisone responsive AR (AR^{ccr}).[5] The physiological concentrations of free cortisol and cortisone in men greatly exceed the binding affinity of AR^{ccr}. The receptor then gets activated, therefore promoting proliferation of prostate cancer cells even in the absence of androgen. The data of Zhao et al.[5] reveal a previously unknown mechanism for the androgen-independent growth of advanced prostate cancer.

A threonine at position 877 in the AR is unique among all human steroid receptors. In contrast to Thr877, Leu701 is a moderately conserved residue among steroid receptors and only found in the progesterone, androgen, and mineralocorticoid receptor. A single Thr877Ala mutation has been reported in advanced prostate cancer[8] and has been well characterized in LNCaP cells.[9] This mutation broadens the ligand specificity by allowing non-androgens such as progesterone, 17β-estradiol, and some anti-androgens such as hydroxyflutamide to act as AR agonists.[5,9] It is worth mentioning that cortisol does not bind or activate the T877A mutant. On the other hand, the single mutation L701H significantly impairs the ability of AR to bind 5α-dihydro-testosterone (DHT), but the same mutation also confers the AR a new phenotype, that is, the L701H mutant responds to cortisol. Interestingly, the AR^{ccr} (L701H and T877A) exhibits a much greater binding affinity for DHT than the L701H mutant, indicating that T877A partially rescues the defect of L701H in DHT binding. Furthermore, in the AR^{ccr}, the transactivation response in the presence of cortisol is much more pronounced in comparison to the L701H mutant, indicating a combined effect of the two mutations. Hence, the AR^{ccr} with its L701H and T877A mutations combines the properties of both single mutants: it renders the receptor responsive to androgens, 17β-estradiol, progesterone, and the anti-androgen hydroxyflutamide and even more responsive to cortisol than the L701H single mutant. It is unknown how these two mutations interact and exert this combined effect on AR function. To understand the structural basis for the glucocorticoid activation of AR^{ccr}, we determined the three-dimensional structure of AR^{ccr} in complex with an agonist. Among 30 natural and synthetic corticosteroids tested, including cortisol and cortisone, 9α-fluorocortisol was found to be the best

* Correspondence should be addressed to Prof. Maria Arménia Carrondo, ITQB-UNL, Av. República, EAN, Apartado 127, P-2781-901 OEIRAS, Portugal. Phone: +351-21-446-9657. Fax: +351-21-443-3644. E-mail: carrondo@itqb.unl.pt.
[†] Universidade Nova de Lisboa.
[‡] Instituto de Biologia Experimental e Tecnológica.
[#] Berlex Biosciences.
[§] Schering AG Research Laboratories.

10.1021/jm011072j CCC: $22.00
Published on Web 02/26/2002

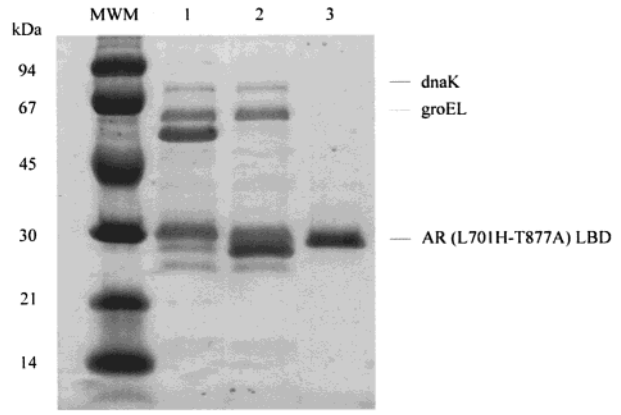

Figure 1. Purification of the AR^{ccr} LBD (L701H and T877A): marker proteins (MWM, size in kDa), 12% SDS−PAGE, Coomassie stained, diluted glutathione sepharose eluate, 10 μL out of 320 mL (1), diluted glutathione eluate after thrombin cleavage, 10 μL out of 320 mL (2), combined fractions of the fractogel eluate, 10 μL out of 51 mL (3).

agonist for the AR^{ccr} with a relative binding affinity (RBA) of 300 as compared to the RBA of 100 of cortisol (Zhao et al., unpublished data). Therefore, we used 9α-fluorocortisol as agonist in the crystal structure analysis of the AR^{ccr}.

The crystal structures of the AR LBD in complex with metribolone (R1881) (**1**),[10] DHT,[11] and the mutant T877A LBD with DHT[11] have been described previously. Herein we present the structure of the double mutant (L701H and T877A) AR^{ccr} LBD in complex with 9α-fluorocortisol (**2**). In addition, energy minimization studies with progesterone, 17β-estradiol, and hydroxyflutamide, an antagonist for the wild-type AR, were performed and may increase our understanding in how these ligands bind and pave the way for the development of new treatments for a subset of androgen-independent prostate cancers harboring AR mutations.

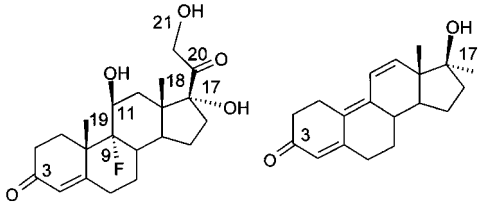

(1) (2)

Results and Discussion

AR^{ccr} LBD Expression and Purification. The AR^{ccr} LBD was successfully expressed in the *Escherichia coli* strain BL21 (DE3) in the presence of 9α-fluorocortisol. In case of the AR (wild-type)-LBD, the expression of a soluble glutathione-S-transferase fusion protein strongly depends on the presence of an agonist during fermentation and purification.[10] In contrast to the wild-type AR-LBD, we were able to express and purify substantial amounts of the AR^{ccr} LBD in the absence of ligand even after cleavage of the fusion protein by thrombin. But only a minor fraction exhibits binding activity toward metribolone (R1881, a stable androgen) after cation exchange chromatography (data not shown). This might indicate a slightly different protein behavior of the AR double mutant. A typical purification of the AR^{ccr} LBD is illustrated in Figure 1. The AR^{ccr} LBD is coeluting from the glutathione sepharose in a complex consisting of the *E. coli* chaperonins GroEL and DnaK as verified by N-terminal sequencing. The heat shock proteins and the remaining thrombin were separated by a cation exchange chromatography resulting in a single band consisting of pure AR^{ccr} LBD. As described for the wild-type AR LBD purification,[10] any protein oxidation was avoided by purging all buffers with nitrogen and by using DTT as an antioxidant.

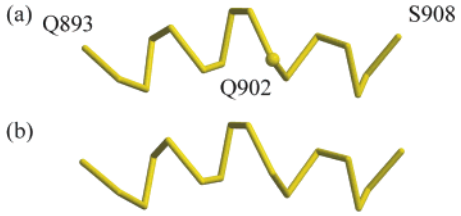

Figure 2. Diagram showing the bend in helix H12 at residue Gln902: (a) AR^{ccr} LBD complexed with 9α-fluorocortisol; (b) T877A hAR LBD mutant complexed with DHT (PDB entry 1i37). Figure produced with MOLSCRIPT[43] and Raster3D.[44]

Structure Analysis. The overall fold of the AR^{ccr} LBD−9α-fluorocortisol complex is very similar to that of the AR LBD−R1881 structure[10] and other similar molecules. On the basis of the secondary structure calculated with PROCHECK according to the Kabsch and Sander algorithm,[12] the structure of the AR^{ccr} LBD−9α-fluorocortisol complex contains nine α-helices, two 3_{10} helices, and four short β-strands associated in two antiparallel β-sheets. The helices are arranged in the typical 'helical sandwich' pattern,[10,13] and helices H4, H5 and H10, H11 are contiguous. As in hAR LBD−R1881, helix H12 seems to be split into two shorter helical segments, with nine and five residues each, respectively. Although PROCHECK apparently failed to reveal this aspect in some closely related three-dimensional structures such as the structures of AR LBD (wild type and T877A mutant) complexed with DHT[11] as well as the hPR LBD−R1881 structure,[10] a visual inspection of these structures on a graphics workstation clearly shows a bending of helix H12 in the same place as in the AR^{ccr} LBD−9α-fluorocortisol complex. This is illustrated in Figure 2 for the structures of AR^{ccr} LBD−9α-fluorocortisol and the T877A AR LBD mutant complexed with DHT.

The structure was analyzed with PROCHECK,[14] and its stereochemical quality parameters were within their respective confidence intervals. In the Ramachandran[15] φ,ϕ plot, 93.2% of the nonglycine and nonproline residues lie within the most favored regions, and no residue is outside the normally allowed regions. In addition, there are only two close contacts (2.5 Å) between Val757 O and Arg760 C$^{\gamma}$ and between Lys845 O and Arg846 N.

The crystal structure coordinates of the AR^{ccr} LBD−9α-fluorocortisol complex were superimposed with those of AR LBD−R1881 using LSQKAB.[16] For the superposition, all the observed main chain atoms in the structure of the AR^{ccr} LBD (see below for details) were used. The rms coordinate deviation was 0.58 Å, again an indication of the highly similar overall fold of these two molecules. The larger main chain rms coordinate deviations (>1.5 Å) are observed in three loop regions—between helices H1 and H3 (residues 691−695), between β-strand S3 and helix H9 (Asp819), and between helices H9 and H10

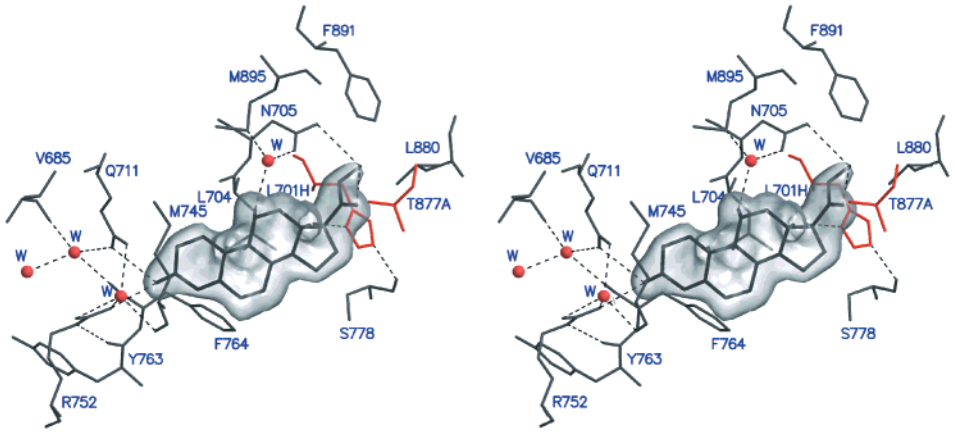

Figure 3. Stereo diagram showing the interactions between the bound 9α-fluorocortisol ligand with the protein chain of the AR^{ccr}-LBD. Residues included are either hydrogen-bonded or have van der Waals contacts with the ligand or nearby residues and water molecules as described in the text. Bound ligand is colored black, conserved residues are colored gray, different residues with respect to wild-type AR LBD are colored red. Dashed lines denote hydrogen bonds (distances given in the text). The surface represents the final $2F_o - F_c$ electron density around the ligand, contoured at the 0.9σ level. Figure produced with MOLSCRIPT,[43] BOBSCRIPT,[45] and Raster3D.[44]

(Arg846 in incomplete loop − see below)—and have no bearing on ligand binding.

Electron density for residues 657−670, 847−850, and 918−919 could not be observed. However, in the N-terminal region of the molecule, some electron density probably corresponding to residues Cys669 and Gln670 was visible, although not with sufficient quality to allow the inclusion of these two residues in the three-dimensional structure. A similar situation was observed for the Thr918 residue in the C-terminal region. Residues 847−850 are located in a loop region linking helices H9 and H10, which is probably very flexible and thus highly disordered in the crystal structure.

The electron density for the ligand 9α-fluorocortisol was very well defined (Figure 3). The conformation of 9α-fluorocortisol in complex with the protein was very similar to its conformation in its own crystal structure[17] as well as the conformation in the single-crystal structures of two corticoid and one cortisone molecules as retrieved from the Cambridge Structural Database.[18−20] The rms deviations of the superimposed atomic coordinates (C5, C10; C8, C9; C13, C14, C17) were below 0.08 Å. The largest conformational deviations were seen in ring A, where the C3═O3 bond showed some degree of directional variability, which was also seen in the different crystal structures and may be attributed to a greater ring flexibility combined with some influence from the molecular vicinity.

Ligand-Binding Pocket Interactions in the Crystal Structure. The hydrogen-bonding scheme in the AR^{ccr} LBD−9α-fluorocortisol complex, in the vicinity of the ligand O3 atom, is similar to that observed between the hAR LBD and R1881.[10] As shown in Figure 3, this oxygen atom forms a hydrogen bond to R752 N$^{\eta 2}$ (2.83 Å), and there is a water molecule near O3 that is hydrogen-bonded to three other residues with a nearly triangular geometry (R752 N$^{\eta,1,2}$ 3.19 and 3.06 Å respectively; M745 O, 2.74 Å; and Q711 O$^{\epsilon 1}$, 2.81 Å). The terminal of the Arg752 side chain is held in place via a hydrogen bond between its N$^{\epsilon}$ atom and Y763 O (3.10 Å). Q711 N$^{\epsilon 2}$ is hydrogen-bonded to a water molecule (3.05 Å) which has further hydrogen bonds to two other residues (V685 O, 2.65 Å and F764 O, 2.84 Å) and a water molecule (2.80 Å) with an overall distorted tetrahedral hydrogen bond geometry. There are, however, two marked differences with the hydrogen-bonding scheme observed between the hAR LBD and R1881: the ligand atom O3 is further hydrogen-bonded to Q711 N$^{\epsilon 2}$ (3.08 Å vs 3.88 Å in the hAR LBD−R1881 complex), and the hydrogen bond between the water molecule near the ligand atom O3 and Arg752 is bifurcated to the terminal N$^{\eta 1}$ and N$^{\eta 2}$ atoms as indicated by the similar distances (3.19 and 3.06 Å), whereas in the hAR LBD−R1881 complex the hydrogen bond was clearly directed toward N$^{\eta 1}$ (2.62 and 3.14 Å).

The 9α-fluorine atom in 9α-fluorocortisol does not form any hydrogen bonds or van der Waals contacts to the protein**.** The shortest distance to the protein is to Leu704 (distance of 3.47 Å to L704 C$^{\delta 2}$) which has a similar side chain conformation in both AR^{ccr} LBD−9α-fluorocortisol and hAR LBD−R1881 complexes. This lack of interaction is a common observation of fluorine atoms in the CSD as well as the PDB databases. An analysis with IsoStar[21,22] showed that only in less than half the structures in the PDB with a fluorine atom in the ligand the fluorine atom is within van der Waals or hydrogen bond distance to the protein atoms. Although making no direct contacts to the protein atoms, the 9α-fluorine atom may contribute to a stronger binding and thus explains the higher affinity of 9α-fluorocortisol to the receptor as compared to that of cortisol and cortisone (RBA of 300 compared to 100 for cortisol and cortisone, respectively).

The 11β-hydroxyl group is present in 9α-fluorocortisol but not in the R1881 ligand. This group is involved in a hydrogen bond with a water molecule (2.74 Å), which has further hydrogen bonds to N705 O$^{\delta 1}$ (2.94 Å) and M895 S$^{\delta}$ (2.95 Å). A hydrogen bond between the sulfur atoms of methionines and hydrogen bond donors is indeed observed in other crystal structures, e.g., in that of the RAR γ-selective ligand BMS184394 and the RXRγ LBD, where the hydroxyl group of the ligand interacts with the S$^{\delta}$ atom of Met727.[23] This water molecule was not observed in the structure of hAR LBD−R1881, presumably due to the lack of a suitable hydrogen bond partner. However, in the structure of hAR LBD−R1881

the C^{ϵ} atom of Met895 side chain is located near the position of this water molecule in the structure of the AR^{ccr} LBD−9α-fluorocortisol complex. A similar situation occurs for the 19α methyl group in 9α-fluorocortisol, which causes the side chain of Met 745 to take a different position in order to avoid an unfavorable van der Waals contact.

The interactions involving the side chains at position 17 in the D-ring of 9α-fluorocortisol are a clear reflection of the different chemical nature of these side chains combined with the double mutation (L701H and T877A) in the protein chain with respect to the native form and explain the ability of the AR^{ccr} LBD to bind 9α-fluorocortisol. As illustrated in Figure 3, the 17α hydroxyl group is hydrogen-bonded to H701 $N^{\delta 1}$ (2.86 Å), a suitable orientation of the imidazole ring being promoted by the hydrogen bond between H701 $N^{\epsilon 2}$ and S778 O (2.57 Å). His 701 clearly makes a strong contribution to the ligand binding in the D-ring region, since this polar interaction would not be possible with a Leucine side chain in the wild-type AR. O21 accepts a hydrogen bond from N705 $N^{\delta 2}$ and makes close van der Waals contacts with L 880 $C^{\delta 2}$ (2.71 Å) and F891 C^{ζ} (3.12 Å). Finally, O20 is the most likely acceptor of an intramolecular hydrogen bond with the O21 hydroxyl group (2.68 Å) and makes close van der Waals contacts with Ala 877 (2.89 Å to C^{β}, 2.91 Å to C^{α}). The presence of a threonine residue instead of an alanine at position 877 would render these van der Waals contacts extremely unfavorable and hence inhibit the binding of 9α-fluorocortisol. Overall, in the double mutant structure there are five hydrogen bonds between the ligand and the protein (two in ring A, one in ring C, and two in ring D) whereas in the complexes between the wild-type AR with either R1881[10] or DHT[11] there are only three (one in ring A and two in ring D). This stronger binding of the of 9α-fluorocortisol ligand to the hAR double mutant may well explain its observed higher affinity for cortisol/cortisone ligands.[5]

Modeling of Ligands in the Ligand-Binding Pocket. The crystal structure of the AR^{ccr} LBD−9α-fluorocortisol complex was subjected to energy minimization calculations to test if the energy minimization protocols used would reproduce the experimental structure. Distance restraints were applied in the calculations to reproduce the hydrogen bond network around the 3-keto group of the ligand (to Arg752, Gln711, and a water molecule, which is conserved in all steroid receptor LBD crystal structures). No restraints were put on the second water molecule in the binding pocket near the 11β-OH group of the ligand. In the energy-minimized AR^{ccr} LBD−9α-fluorocortisol complex, a hydrogen bond network was obtained involving the 11β-OH group of the ligand and the oxygen atom of the water molecule similar to that observed in the crystal structure. A water molecule at a similar position in the LBD of the glucocorticoid receptor (GR) might explain the selectivity of glucocorticoids with an 11β-hydroxyl group.

The size of the binding niche of the AR^{ccr} LBD near the D-ring of steroidal ligands is increased with respect to the wild-type structure due to the substitution of a threonine by an alanine and of a leucine by an histidine. Due to this difference in size, ligands such as progesterone, 17β-estradiol, and hydroxyflutamide can be fitted into the LBP. Compared to the wild-type AR, which has a low affinity for binding progesterone as well as estradiol, the affinity of these ligands in the double mutant is markedly increased.[5] From Figure 4 it can be seen that progesterone and estradiol occupy areas in the ligand-binding pocket near Ala877. A threonine at this position would severly interfere with a binding of these ligands to the wild-type AR receptor. Similar to the crystal structure of the hPR LBD−progesterone complex, no polar interactions are observed in the AR^{ccr} LBD−progesterone model complex between the 17β-acetyl group of progesterone and the protein. The actual size of the binding niche is strongly influenced by the orientation of residues lining the binding pocket. This is visualized in Figure 4 as protrusions extending from the main body of the LBP. The planar conformation of His701 side chain explains the observed protrusion in the LBP of the double mutant below the steroidal scaffold (Figure 4a,b). The orientation of the Trp741, Met 895, and Ile899 side chains is influencing the size of the binding pocket above the steroidal scaffold, whereas the position of the Ser778 and Met780 side chains determine the size of the niche below the steroidal scaffold.

Hydroxyflutamide can be fitted into the LBP of the AR^{ccr} as an agonist, in an orientation similar to that published by Marhefka et al.[24] The oxygen atoms of the nitro moiety are hydrogen-bonded to Arg752 and Gln711, while the hydroxyl group of the ligand is interacting with Asn705. Hydroxyflutamide fits tightly into the LBP of the AR^{ccr} LBD. The LBP of the wild-type AR LBD is smaller in the plane of a steroidal ligand than that of the AR^{ccr} LBD, and hydroxyflutamide would fit too tightly into the wild-type LBP. In other nuclear receptor LBDs, e.g., those in the retinoic acid receptor (RAR) family, it has been observed that agonist ligands adapt to the ligand binding pocket while the protein conformation is conserved.[23,25] A superposition of all available AR LBD structures indeed shows a remarkable conserved conformation of these crystal structures. A similar effect like in the RAR family might be hypothesized for the wild-type AR, where hydroxyflutamide would fit too tightly into the LBP. To decrease the structural constraints of the ligand on the receptor, the conformation of the LBD has to accommodate to the ligand most likely by a change of the orientation of helix H12 similar to that seen in the crystal structures of estrogen receptor LBD−antagonist complexes.[26−28] Therefore, hydroxyflutamide would function as an antagonist rather than an agonist in the wild-type AR.

The crystal structure of the AR^{ccr} LBD quite nicely supports the biochemical observations of agonistic activities (binding and transactivation) of 9α-fluorocortisol, 17β-estradiol, progesterone, and hydroxyflutamide at an atomic level which is important for the development of new AR antagonists for androgen-independent prostate cancer.

Experimental Section

Site-Directed Mutagenesis. Mutations were created in the wild-type hAR LBD cDNA (aa663-aa919) in pGEX-KG-AR-LBD. The hAR LBD inserted into the expression vector pGEX-KG[29] was previously described.[10] The mutants were generated using a QuikChange Site-Directed Mutagenesis Kit (Stratagene). The mutagenic oligonucleotides (MWG-Biotech

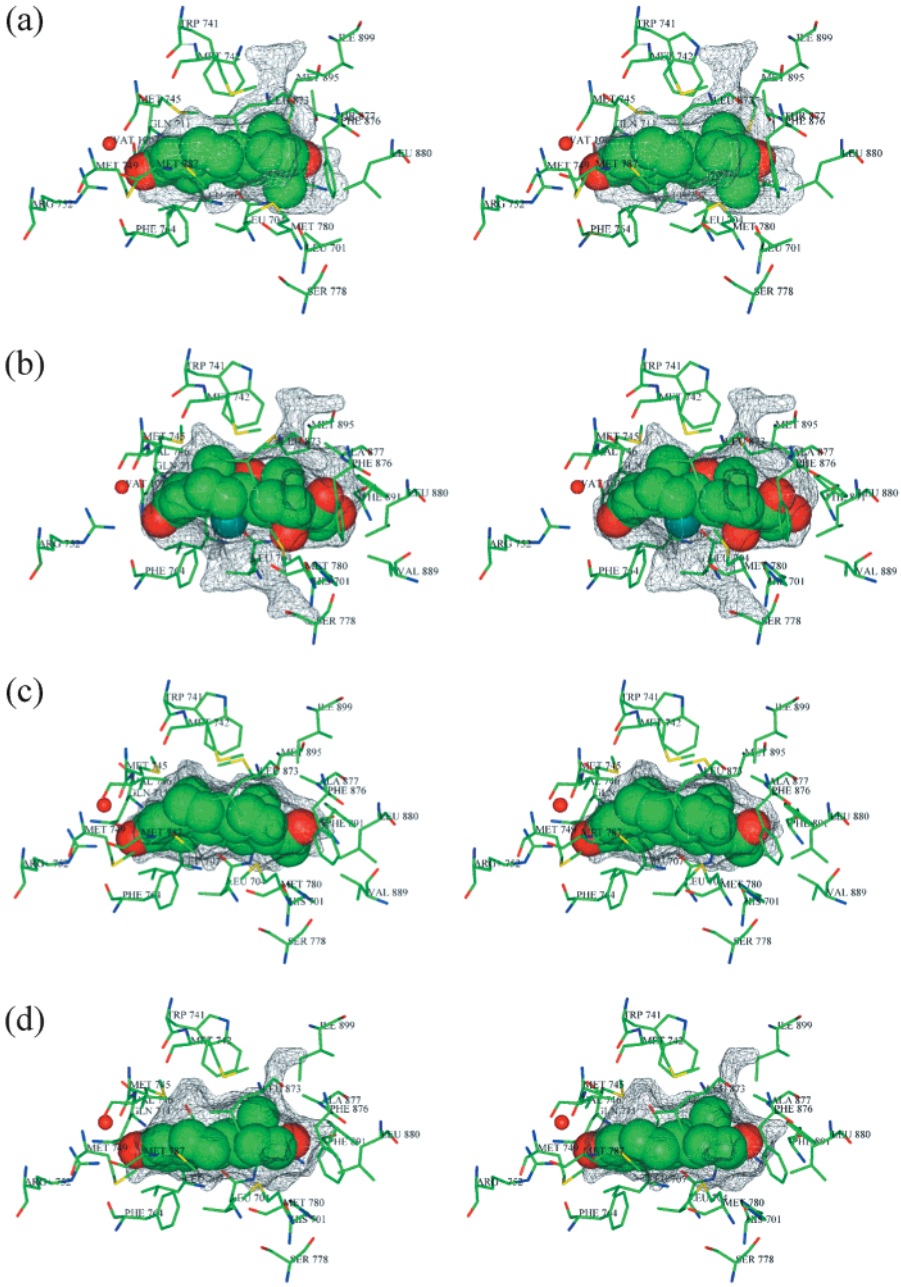

Figure 4. Stereo diagram showing the LBP with all amino acid residues within 4 Å around the respective ligand. The size of the binding niche is shown as a gray surface calcultated with the binding site module of Insight2000 (Accelrys, San Diego, CA): (a) crystal structure of the wild-type AR LBD−R1881 complex, (b) crystal structure of the AR^{ccr} LBD−9α-fluorocortisol complex, (c and d) model structure of the AR^{ccr} LBD in complex with progesterone and 17β-estradiol, respectively.

AG, Ebersberg, Germany) used were 5-CGACTCCTTTG-CAGCCTTGCACTCTAGCCTCAATGAACTGG-3′ (forward primer) and 5′-CCAGTTCATTGAGGCTAGAGTGCAAGGCT-GCAAAGGAGTCG-3′ (reverse primer) for L701H and 5′-GAGAGAGCTGCATCAGTTCGCTTTTGACCTGCTAATCAAG-3′ (forward primer) and 5′-CTTGATTAGCAGGTCAAAAGC-GAACTGATGCAGCTCTCTCG-3′ (reverse primer) for T877A (mutated bases are underlined). Final constructs were sequenced to confirm the mutations.

Protein Expression and Purification. Fermentation using the corresponding rec *E. coli* strain expressing the hAR LBD (L701H and T877A) double mutant was carried out in 2XYT medium in the presence of ampicillin (200 μg/mL) supplemented with 10 μM 9α-fluorocortisol. Expression was induced with 10 μM IPTG (isopropyl-β-D-thiogalactoside), and the fermentation (10 L) was continued at 15 °C for 16 h. Cells were harvested by centrifugation and disrupted twice in a continuous high pressure homogenizer (9000 psi) in a buffer containing 50 mM Tris-HCl, pH 8, 150 mM NaCl, 5 mM EDTA, 10% glycerol, 100 μM 9α-fluorocortisol, 100 μM PMSF, and 10 mM DTT. All buffers were purged with nitrogen for 1 h before adding DTT. The supernatants were loaded onto a glutathione sepharose column and washed with 50 mM Tris-HCl, pH 8, 150 mM NaCl, 5 mM EDTA, 10% glycerol, 10 μM 9α-fluorocortisol, 0.1% *n*-octyl-β-glucoside, and 1 mM DTT, and the fusion protein was eluted using the same buffer supplemented with 15 mM reduced glutathione. The eluate was diluted with 100 mM HEPES pH 7.2, 150 mM NaCl, 0.5 mM EDTA, 10% glycerol, 10 μM 9α-fluorocortisol, 1 mM DTT, and 0.1% *n*-octyl-β-glucoside up to a fusion protein concentration of 0.75 mg/mL. A thrombin cleavage (2 N.I.H. units/mg fusion protein) was performed for 5 h at 22 °C. The protein mixture was further diluted 3-fold with 10 mM HEPES pH 7.2, 10% glycerol, 10 nM 9α-fluorocortisol, 10 mM DTT, and 0.1% *n*-octyl-β-glucoside and loaded onto a Fractogel SO_3^- column (Merck) and eluted with a gradient of 50−500 mM NaCl in a 10 mM HEPES buffer pH 7.2, 10% glycerol supplemented with 10 nM 9α-fluorocortisol, 10 mM DTT, and 0.1% *n*-octyl-β-

Table 1. Summary of Crystallographic Data Collection and Refinement for AR^{ccr}-LBD−9α-Fluorocortisol

Crystallographic Data		
data set	ESRF ID14-EH1	ESRF ID14-EH2
space group	$P2_12_12_1$	$P2_12_12_1$
unit cell [Å]		
a	55.80	56.35
b	66.23	66.24
c	72.99	73.06
detector	MAR CCD 165 mm	ADSC Quantum 4
wavelength [Å]	0.934	0.933
resolution range [Å]	19.8−2.25	21.5−1.95
observations (unique reflections)	52 277 (13 248)	74 323 (20 515)
% completeness[a]	99.9 (99.9)	99.9 (100.0)
redundancy	3.9	3.6
R_{merge}[a,b]	0.040 (0.283)	0.045 (0.266)
$I/\sigma(I)$ (estimated $B_{overall}$)	15.5 (44.3)	22.7 (30.0)
Refinement		
final % *R*-factor (% *R*-free) [all data][c]		20.5 (28.5)
final % *R*-factor (% *R*-free) [$I > 2\sigma(I)$][c]		19.7 (27.2)
non-hydrogen atoms		
protein (missing)[d]		1992 (22)
ligand		27
solvent		111
rmsd on bond lengths (bond angles) [Å][e]		0.005 (0.020)
estimated overall rms coordinate error [Å][f]		0.18
average *B* values for non-hydrogen atoms [Å^2]		
protein main chain (side chain)		30.5 (37.2)
ligand (water)		30.7 (34.5)

[a] Values in parentheses refer to the last resolution shell, $2.33 \geq d \geq 2.25$ Å for the ID14-EH1 data set and $2.00 \geq d \geq 1.95$ Å for the ID14-EH2. [b] $R_{merge} = \Sigma_{hkl}\Sigma_i|I_{hkl,i} - \langle I_{hkl}\rangle|/\Sigma_{hkl}\Sigma_i|I_{hkl,i}|$ with $\langle I_{hkl}\rangle$ the mean intensity of the set of symmetry-related reflections denoted by $I_{hkl,i}$. [c] *R*-factor $= \Sigma_{hkl}|F_{obs} - F_{calc}|/\Sigma_{hkl}|F_{obs}|$ for all $|F_{obs}|$ in the working set. *R*-free is calculated in a similar fashion using all $|F_{obs}|$ in the test set. [d] The number of missing atoms refers to the model coordinates with zero occupation factor (see Discussion). [e] SHELXL-97 defines bond angles in terms of 1,3 interatomic distances. [f] Calculated with SIGMAA.[41,42]

glucoside. Approximately 1.5 mg of purified hAR LBD can be recovered from 1 L of *E. coli* cell culture. Protein concentration was determined with Bio-Rad protein assay. Aliquots of the purified protein with a concentration of 0.3 mg/mL were frozen in liquid N_2 under N_2 atmosphere and stored at −80 °C.

Crystallization, Data Collection, and Structure Determination. The buffer in the purified protein solution was exchanged by washing with a solution containing 10 mM HEPES pH 7.2, 0.1% *n*-octyl-β-glucoside, 10% glycerol, 10 nM 9α-fluorocortisol, 150 mM Li_2SO_4, 10 mM DTT, and 1 mM EDTA and concentrated in a 3 mL Amicon minicell up to 6.5 mg/mL. The AR^{ccr} LBD in complex with 9α-fluorocortisol was crystallized using the sitting drop vapor diffusion method at 20 °C. The largest crystals were obtained in drops composed of 3 μL of protein plus 1 or 2 μL of reservoir solution. The two reservoir solutions that produced good results contained 0.4 M $Na_2HPO_4{\cdot}2(H_2O)$, 0.4 M K_2HPO_4, 0.1 M Tris-maleate pH 9.5, 5% PEG 200, or 0.4 M $Na_2HPO_4{\cdot}2(H_2O)$, 0.4 M K_2HPO_4, 0.1 M Tris-HCl pH 8.5, 0.1 M $(NH_4)_2HPO_4$, and 1% ethanol. Crystals appeared within 2 days and grew during 4 more days to dimensions of $0.06 \times 0.06 \times 0.25$ mm^3. The crystals were flash frozen in a 0.4 M $Na_2HPO_4{\cdot}2(H_2O)$, 0.4 M K_2HPO_4, 0.1 M Tris-HCl pH 8.5, 0.1 M $(NH_4)_2HPO_4$, 25% glycerol solution.

Data were collected from two flash cooled crystals at the ESRF (Grenoble, France) on two separate occasions: the first at beamline ID14-EH1 to a resolution of 2.25 Å and later another data set was collected at beamline ID14-EH2 to a resolution of 1.95 Å. Both data sets were integrated and reduced using DENZO and SCALEPACK.[30] Statistics of X-ray data collection and processing are summarized in Table 1.

The AR^{ccr} LBD−9α-fluorocortisol complex crystallized in the same orthorhombic space group $P2_12_12_1$ and with similar cell parameters as the AR LBD−R1881 complex[10] and also with one monomer in the asymmetric unit. The structure determination for the AR^{ccr} LBD−9α-fluorocortisol complex was carried out using the molecular replacement method in AMoRe[31] with the coordinates of the AR LBD molecule in the AR LBD−R1881 complex as the search model. A clear solution was obtained using data between 15.0 and 3.5 Å from the first (2.25 Å) data set.

Refinement of AR^{ccr} LBD−9α-Fluorocortisol Complex. The molecular replacement solution obtained was initially refined using X-PLOR[32] and the first data set to 2.25 Å resolution. In all refinements and map calculations with X-PLOR, a bulk solvent correction was used and all low resolution data were included. Prior to the refinement calculations, a random 5% sample of the reflection data was flagged for *R*-free calculations.[33] All model interactive visualization and editing was carried out using TURBO.[34] The fast wARP[35,36] molecular replacement protocol was also applied after the first few XPLOR refinements in an attempt to further improve the $2|F_o| - |F_c|$ electron density map. Prior to its inclusion in the model, the electron density for the 9α-fluorocortisol ligand was clearly visible in all maps. A model for the ligand was obtained from the Cambridge Structural Database entry FPRTOD10.[17,21] The XPLOR topology and parameter dictionaries were built using program XPLO2D.[37] The refinement was continued with program SHELXL-97[38] using the second data set to 1.95 Å resolution. In this data set, care was taken to ensure that the same reflections were used for *R*-free calculations up to 2.25 Å resolution as in the first data set. The dictionary of geometrical restraints for the ligand was built by inspection, using the coordinates from the last XPLOR refinement. In the final refinement at 1.95 Å, 106 water molecules and one PO_4^{2-} ion were included in the model, and individual restrained *B*-factors were refined for all non-hydrogen atoms. The occupation factors of 47 water molecules and the PO_4^{2-} ion were arbitrarily set to 0.5 because in the course of the refinement their thermal motion parameters (*B*) became larger than about 50 Å^2. A 2-fold disorder model was included in the refinement for Cys806, and the occupation factors of the major and minor components converged to 0.58 and 0.42, respectively. The final values of *R* and *R*-free were 20.5% and 28.5%, respectively. The main refinement results and statistics are shown in Table 1. Coordinates of the refined three-dimensional structure have been deposited with the Protein Data Bank[39,40] with PDB accession code 1gs4.

Energy Minimization of AR^{ccr} LBD−Ligand Complexes. In the crystal structure of the AR^{ccr} LBD (residues 670−917), poor electron density was observed for residues 847−850 (see discussion below), a loop region far away from the ligand-binding pocket. To obtain a contiguous LBD, the residues in this loop region were substituted by the equivalent loop region of the wild-type AR LBD (PDB entry 1e3g). In the

final model, residues 839−851 were taken from the wild-type structure to obtain a loop region with main chain torsion angles in the allowed regions of the Ramachandran plot. One water molecule in the LBD of the double mutant near Lys854 had to be deleted due to the close distance to this residue. Residue His917 was chosen to have the hydrogen atom on the N^{δ} atom.

The energy minimization calculations on the AR^{ccr} LBD were performed similarly to that of the wild-type AR LBD with respect to the programs used and the refinement protocol applied.[10] During the energy minimizations, the hydrogen network around the 3-keto group of the ligands were fixed as observed in the crystal structure. Initially, ligands other than 9α-fluorocortisol were manually adjusted into the LBP with hydrogen bonds to Arg752. All complexes including the crystallographically determined water molecules were soaked with a 12 Å layer of water and were subjected to force field energy minimizations using the CFF91 force field (Discover 2.97 from Accelrys, San Diego, CA; http://www.accelrys.com/insight/discover.html). Dihedral angles in progesterone defined by the atoms (C18−C13−C17−C20) were forced to −46°, (C20−C17−C16−C15) to 143°, (C16−C17−C20−O20) to −6.5°, and (C16−C17−C20−C21) to 171°, respectively, during the calculations using a force constant of 100 kcal rad^{-2}. In the energy minimization of the AR^{ccr} LBD−9α-fluorocortisol complex, the C^{α}-atoms of residues 670−840 and 854−917 were fixed to their original positions to maintain the overall structure of the LBD. In the calculations with other ligands, all C^{α} atoms were fixed except those within a 5 Å sphere around the ligand. The energies of the models were minimized until the maximum derivative was less than 0.5 kcal (Å)$^{-1}$. Models were evaluated using stereochemical criteria and by visual inspection (PROCHECK).[14]

Acknowledgment. We thank Norbert Otto (Schering AG, Berlin) for helpful discussions and Werner Boidol (Schering AG Berlin) for fermentation. Thanks are also due to the ESRF (Grenoble, France) for financial and technical support for X-ray diffraction data collection experiments.

References

(1) Visakorpi, T.; Hyytinen, E.; Koivisto, P.; Tanner, M.; Keinanen, R.; et al. In vivo amplification of the androgen receptor gene and progression of human prostate cancer. *Nat. Genet.* **1995**, *9*, 401−406.

(2) Brinkmann, A. O.; Trapman, J. Prostate cancer schemes for androgen escape. *Nat. Med.* **2000**, *6*, 628−629.

(3) Tablin, M. E.; Bubley, G. J.; Shuster, T. D.; Frantz, M. E.; Spooner, A. E.; et al. Mutation of the androgen receptor gene in metastatic androgen independent prostate cancer. *New Engl. J. Med.* **1995**, *332*, 1393−1398.

(4) Zhao, X. Y.; Boyle, B.; Krishnan, A. V.; Navone, N. M.; Peehl, D. M.; et al. Two mutations identified in the androgen receptor of the new human prostate cancer cell line MDA PCa 2a. *J. Urol.* **1999**, *162*, 2192−2199.

(5) Zhao, X. Y.; Malloy, P. J.; Krishnan, A. V.; Swami, S.; Navone, N. M.; et al. Glucocorticoids can promote androgen-independent growth of prostate cancer cells through a mutated androgen receptor. *Nat. Med.* **2000**, *6*, 703−706.

(6) Zhao, X. Y.; Peehl, D. M.; Navone, N. M.; Feldman, D. 1alpha,-25-dihydroxyvitamin D3 inhibits prostate cancer cell growth by androgen-dependent and androgen-independent mechanisms. *Endocrinology* **2000**, *141*, 2548−2556.

(7) Navone, N. M.; Olive, M.; Ozen, M.; Davis, R.; Troncoso, P.; et al. Establishment of two human prostate cancer cell lines derived from a single bone metastasis. *Clin. Cancer Res.* **1997**, *3*, 2493−2500.

(8) Gaddipati, J. P.; McLeod, D. G.; Heidenberg, H. B.; Sesterhenn, I. A.; Finger, M. J.; et al. Frequent detection of codon 877 mutation in the androgen receptor gene in advanced prostate cancers. *Cancer. Res.* **1994**, *54*, 2861−2864.

(9) Veldscholte, J.; Voorhorst-Ogink, M. M.; Bolt-de Vries, J.; van Rooij, H. C.; Trapman, J.; et al. Unusual specificity of the androgen receptor in the human prostate tumor cell line LNCaP: high affinity for progestagenic and estrogenic steroids. *Biochim. Biophys. Acta* **1990**, *1052*, 187−194.

(10) Matias, P. M.; Donner, P.; Coelho, R.; Thomaz, M.; Peixoto, C.; et al. Structural evidence for ligand specificity in the binding domain of the human Androgen receptor: implications for pathogenic gene mutations. *J. Biol. Chem.* **2000**, *275*, 26164−26171.

(11) Sack, J. S.; Kish, K. F.; Wang, C.; Attar, R. M.; Kiefer, S. E.; et al. Crystallographic structures of the ligand-binding domains of the androgen receptor and its T877A mutant complexed with the natural agonist dihydrotestosterone. *Proc. Natl. Acad. Sci. U.S.A.* **2001**, *98*, 4904−4909.

(12) Kabsch, W.; Sander, C. Dictionary of protein secondary structure: pattern recognition of hydrogen-bonded and geometrical features. *Biopolymers* **1983**, *22*, 2577−2637.

(13) Williams, S. P.; Sigler, P. B. Atomic structure of progesterone complexed with its receptor. *Nature* **1998**, *393*, 392−396.

(14) Laskowski, R. A.; MacArthur, M. W.; Moss, D. S.; Thornton, J. M. PROCHECK − a program to check the stereochemical quality of proteins. *J. Appl. Crystallogr.* **1993**, *26*, 283−291.

(15) Ramachandran, G. N.; Sasisekharan, V. Conformation of polypeptides and proteins. *Adv. Protein Chem.* **1968**, *23*, 283−437.

(16) Kabsch, W. A solution for the best rotation to relate two sets of vectors. *Acta Crystallogr.* **1976**, *A32*, 922−923.

(17) Dupont, L.; Dideberg, O.; Campsteyn, H. Structure cristalline et moléculaire du 9α-fluorocortisol, $C_{21}H_{29}O_5F$. *Acta Crystallogr.* **1972**, *B28*, 3023−3032.

(18) Declercq, J. P.; Germain, G.; van Meerssche, M. Cortisone. *Cryst. Struct. Commun.* **1972**, *1*, 13.

(19) Roberts, P. J.; Coppola, J. C.; Isaacs, N. W.; Kennard, O. Cortisol methanol solvate. (11*β*,17α,21-Trihydroxy-pregn-4-ene-3,20-dione methanol solvate). *J. Chem. Soc., Perkin Trans. 2* **1973**, 774.

(20) Campsteyn, H.; Dupont, L.; Dideberg, O. Solvate 1:1 cortisol-pyridine, $C_{21}H_{30}O_5 \cdot C_5H_5N$. *Acta Crystallogr.* **1974**, *B30*, 90−94.

(21) Allen, F. H.; Bellard, S.; Brice, M. D.; Cartwright, B.; Doubleday, A.; et al. Cambridge Structural Database. *Acta Crystallogr.* **1979**, *B35*, 2331−2339.

(22) Bruno, I. J.; Cole, J. C.; Lommerse, J. P. M.; Scott Rowland, R.; Taylor, R.; et al. IsoStar: A library of information about nonbonded interactions. *J. Comput.-Aided Mol. Des.* **1997**, *11*, 525−537.

(23) Klaholz, B. P.; Mitschler, A.; Belema, M.; Zusi, C.; Moras, D. Enantiomer discrimination illustrated by high-resolution crystal structures of the human nuclear receptor hRAR*γ*. *Proc. Natl. Acad. Sci. U.S.A.* **2000**, *97*, 6322−6327.

(24) Marhefka, C. A.; Moore, B. M.; Bishop, T. C.; Kirkovsky, L.; Mukherjee, A.; et al. Homology modeling using multiple molecular dynamics simulations and docking studies of the human androgen receptor ligand binding domain bound to testosterone and nonsteroidal ligands. *J. Med. Chem.* **2001**, *44*, 1729−1740.

(25) Egea, P. F.; Klaholz, B. P.; Moras, D. Ligand-protein interactions in nuclear receptors of hormones. *FEBS Lett.* **2000**, *476*, 62−67.

(26) Shiau, A. K.; Barstad, D.; Loria, P. M.; Cheng, L.; Kushner, P. J.; et al. The structural basis of estrogen receptor/coactivator recognition and the antagonism of this interaction by tamoxifen. *Cell* **1998**, *95*, 927−937.

(27) Brzozowski, A. M.; Pike, A. C. W.; Dauter, Z.; Hubbard, R. E.; Bonn, T.; et al. Molecular basis of agonism and antagonism in the oestrogen receptor. *Nature* **1997**, *389*, 753−758.

(28) Pike, A. C.; Brzozowski, A. M.; Walton, J.; Hubbard, R. E.; Thorsell, A.; et al. Structural Insights into the Mode of Action of a Pure Antiestrogen. *Structure (Camb)* **2001**, *9*, 145−153.

(29) Guan, K. L.; Dixon, J. E. Eukaryotic proteins expressed in *Escherichia coli*: an improved thrombin cleavage and purification procedure of fusion proteins with glutathione S-transferase. *Anal. Biochem.* **1991**, *192*, 262−267.

(30) Otwinowski, Z.; Minor, W. Processing of X-ray diffraction data collected in oscillation mode. *Macromolecular Crystallography part A*; Academic Press: New York, 1997; pp 307−326.

(31) Navaza, J. AMoRe: an automated package for molecular replacement. *Acta Crystallogr.* **1994**, *A50*, 157−163.

(32) Brünger, A. T. *X-PLOR: a system for Crystallography and NMR*; The Howard Hughes Medical Institute and Department of Molecular Biophysics and Biochemistry, Yale University: New Haven, CT, 1992.

(33) Brünger, A. T. Free *R* value: A novel statistical quantity for assessing the accuracy of crystal structures. *Nature* **1992**, *355*, 472−474.

(34) Roussel, A.; Fontecilla-Camps, J. C.; Cambillau, C. *TURBO−FRODO: a new program for protein crystallography and modelling*; XV IUCr Congress: Bordeaux, France, 1990; pp 66−67.

(35) Lamzin, V. S.; Wilson, K. S. Automated refinement for protein crystallography. *Macromolecular Crystallography part B*; Academic Press: New York, 1997; pp 269−305.

(36) Perrakis, A.; Sixma, T. K.; Wilson, K. S.; Lamzin, V. S. wARP: improvement and extension of crystallographic phases by weighted averaging of multiple refined dummy atomic models. *Acta Crystallogr.* **1997**, *D53*, 448−455.
(37) Kleywegt, G. J. Dictionaries for Heteros. In *Joint CCP4 and ESF-EACMB Newsletter on Protein Crystallography*; The Daresbury Laboratory: Daresbury, Warrington, U.K., 1995; pp 45−50.
(38) Sheldrick, G. M.; Schneider, T. R. SHELXL: High-resolution refinement. *Macromolecular Crystallography part B*; Academic Press: New York, U.S.A., 1997; pp 319−343.
(39) Bernstein, F. C.; Koetzle, T. F.; Williams, G. J. B.; E. F. M., Jr.; Brice, M. D.; et al. The Protein Data Bank: A computer-based archival file for macromolecular structures. *J. Mol. Biol.* **1977**, *112*, 535−542.
(40) Abola, E. E.; Bernstein, F. C.; Bryant, S. H.; Koetzle, T. F.; Weng, J. Protein Data Bank. *Crystallographic Databases − Information Content, Software Systems, Scientific Applications*; Data Comission of The International Union of Crystallography: Bonn/Cambridge/Chester, 1987; pp 107−132.
(41) Collaborative Computational Project Number 4. The CCP4 suite: programs for protein crystallography. *Acta Crystallogr.* **1994**, *D50*, 760−763.
(42) Read, R. J. Improved Fourier coefficients for maps using phases from partial structures with errors. *Acta Crystallogr.* **1986**, *A42*, 140−149.
(43) Kraulis, P. J. MOLSCRIPT: A program to produce both detailed and schematic plots of protein structures. *J. Appl. Crystallogr.* **1991**, *24*, 946−950.
(44) Merritt, E. A.; Murphy, M. E. P. Raster3D version 2.0. A program for photorealistic molecular graphics. *Acta Crystallogr.* **1994**, *D50*, 869−873.
(45) Esnouf, R. M. Further additions to *MolScript* version 1.4, including reading and contouring of electron-density maps. *Acta Crystallogr.* **1999**, *D55*, 938−940.

JM011072J